Supplementary Materials
Towards Photography Through Realistic Fog

Guy Satat, Matthew Tancik, Ramesh Raskar
MIT Media Lab
guysatat@mit.edu

1. Description of Videos

1. **Overview.mp4**   This is an overview video providing a high-level description of the paper and results.

2. **Es_Over_Time.mp4**   Shows the reconstruction for the 'E's target as fog is being added into the chamber. The video starts with an empty chamber, and ends when the fog level in the chamber saturates. The video shows the PointGrey camera measurements, SPAD photon counts, SPAD time gating, and our reflectance and depth reconstruction. Similarly to Fig. 5 in the main text, we provide SSIM and PSNR for quantitative comparison. Each frame indicates the measured optical thickness.

3. **Mannequin_Close_Over_Time.mp4**   Similar to the above for the mannequin measurements, when the mannequin is 35cm away from the camera.

4. **Mannequin_Far_Over_Time.mp4**   Similar to the above for the mannequin measurements, when the mannequin is 65cm away from the camera.

5. **Optical_Thickness_Over_Time.mp4**   Shows the PointGrey camera perspective for a scene composed of posts separated by 5cm and starting at 27cm away from the camera. Each frame shows the measured optical thickness.

2. Further Experimental Details

Supplemental Fig. 1 shows the dimensions of the 'E' shape target. Our reconstructions in the main text demonstrate recovery with 1cm spatial resolution and 5cm axial resolution for targets at a range of 37-57cm.

3. Extension for Figure 3 from the Main Text

Supplemental Figs. 2+3 provide results on top of Fig. 3 in the main text. Supplemental Fig. 2 shows results that correspond to the left column of Fig. 3 in the main text
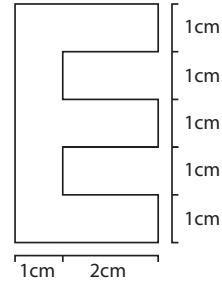

Figure 1. Sketch of the E target. The actual target is composed of four identical E shapes separated by 5cm from one another.

(estimated KDE, Gamma distribution, signal distribution, and target distribution). Supplemental Fig. 3 shows results that correspond to the right column of Fig. 3 in the main text (histogram and fitted model from Eq. 5). Both figures show results for targets at five different depths (42, 47, 52, 57, 62cm), and a background pixel. Both figures shows results for optical thicknesses (OT) of: 0, 1.0, 1.6, 1.9, 2.3, 2.8. All photon counts are normalized to [0,1], and the title of each subplot indicates the total photons measured.

We note that when the object is closer, it can be recovered with more challenging OT. For example the closest object at 42cm is always correctly recovered, the next target at 47cm is correctly recovered up to OT=2.3, and then fails for OT=2.8, and the furthest target (62cm) fails as early as OT=1.6.

We also note that for the background, as soon as little fog is added, the number of counts rises very rapidly, and then stays roughly the same for denser fog (the response shape does change as more fog is added). The opposite process occurs for the targets – as more fog is added, we note less counts.

Lastly, supplemental Fig. 3 shows that the suggested model captures the measurements well at diverse levels of fog (OT) and target depths.
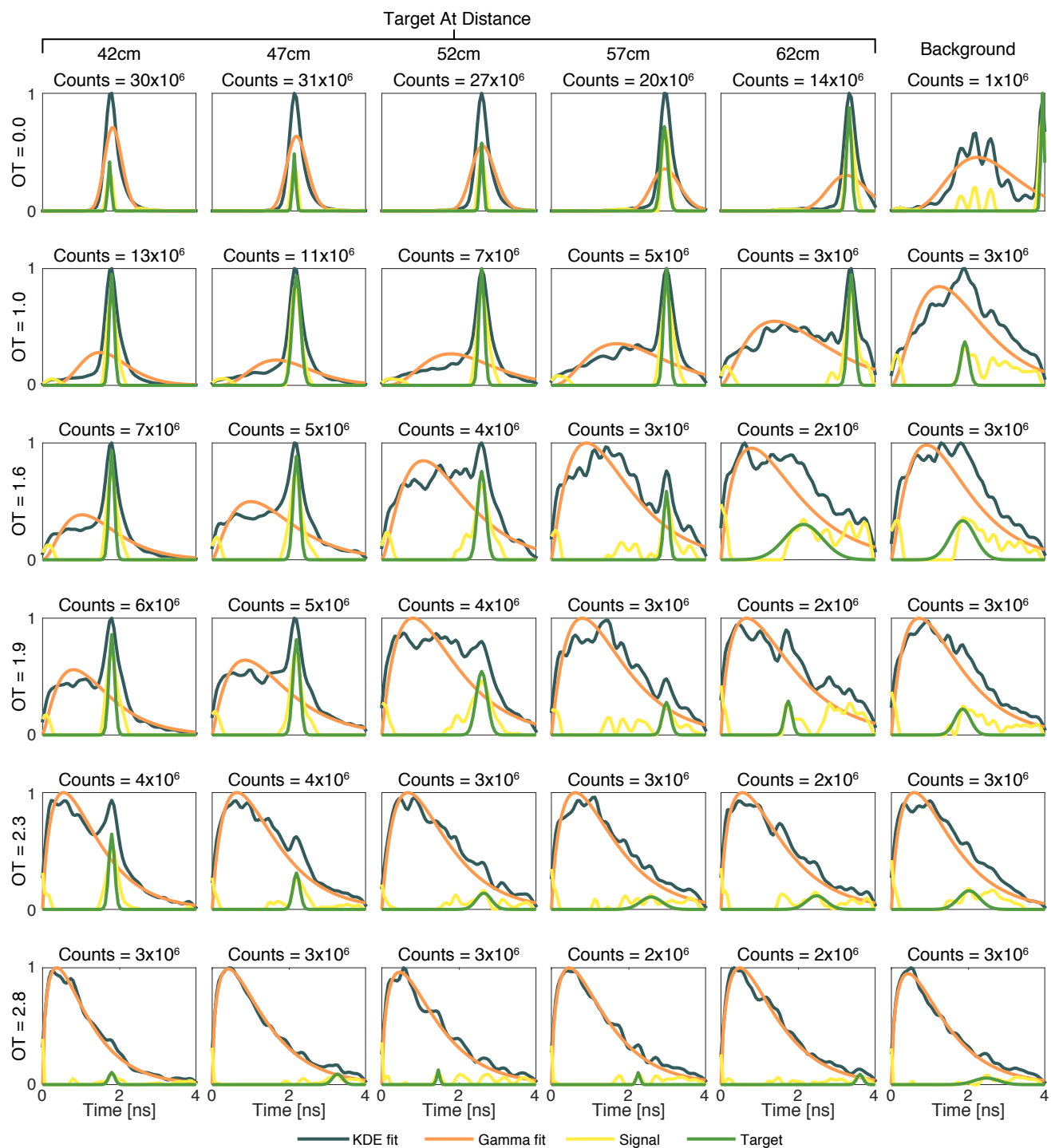
Figure 2. Extension to figure 3 from the main text. Recovered KDE and Gamma distributions (from the raw photon counts), estimated signals by subtracting the two, and estimated target distributions. Rows show different cases of fog concentrations (OT). Columns show different target depths and a space with no target.
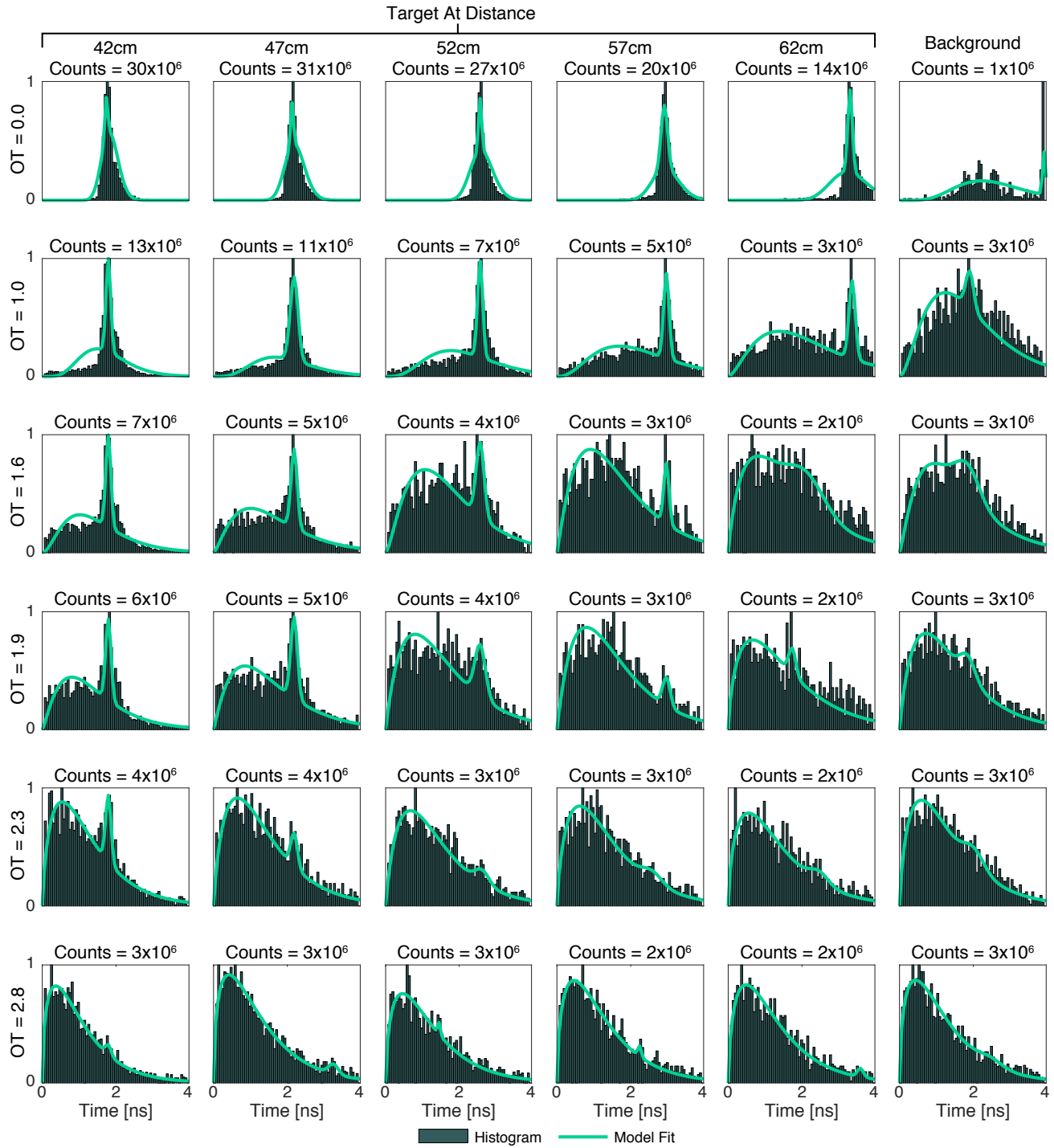
Figure 3. Extension to figure 3 from the main text. Histogram generated by the raw photon counts and the fitted model by Eq. 5. Rows show different cases of fog concentrations (OT). Columns show different target depths and a space with no target.